Cancer cell-derived exosomal miR-34a inhibits the malignant progression of pancreatic adenocarcinoma cells by restraining the M2 polarization of macrophages

Kui Long,[1] Xiang Kui,[2] Qingbin Zeng,[1] Wenzhi Dong[1]

[1]Department of Three Wards of Hepatobiliary Surgery;
[2]Department of Pathology, The Second Affiliated Hospital of Kunming Medical University, Kunming, Yunnan, China

ABSTRACT

This study aimed to investigate the crosstalk mechanism between pancreatic cancer (PAC) cells and M2 tumor-associated macrophages (TAMs) induced by tumor-derived exosomal miR-34a. Micro RNA and mRNA expression levels were detected using RT-qPCR. Cell Counting Kit-8, wound-healing, transwell assays and flow cytometry were respectively employed to assess cell proliferation, migration, invasion and apoptosis. Enzyme-linked immunosorbent assay was utilized to determine cytokine secretion. Transmission electron microscopy and nanoparticle tracking analyses were performed to detect the exosome morphology and particle size. Phagocytosis of exosomes by macrophages was verified by PKH26 labeling. The effects of exosome-treated macrophages on the epithelial-mesenchymal transition, invasion, and migration of PANC-1 cells were investigated using coculture experiments. The identification of miR-34a's potential targets was determined with TargetScan and validated by a dual-luciferase reporter assay. miR-34a was downregulated in PAC tissues, cells, and exosomes. Overexpression of miR-34a inhibited PANC-1 cell malignancy and suppressed M2 macrophage polarization through PANC-1-derived exosomes. This, in turn, restrained the epithelial-mesenchymal transition, migration, and invasion of cocultured PANC-1 cells. Suppressor of cytokine signaling 3 (SOCS3) was identified as a direct target of miR-34a. Mechanistically, miR-34a negatively regulated SOCS3 expression, thereby preventing M2 polarization of macrophages by engaging the Janus kinase/signal transducers and activators of the transcription (JAK/STAT) pathway and influencing the malignancy of PAC cells. These findings highlight the novel role of exosomal miR-34a in modulating the tumor microenvironment by restraining M2 macrophage polarization, thereby impeding PAC progression. Importantly, these results provide novel insights into the therapeutic potential of exosomal miR-34a as a promising target for modulating macrophage function in the tumor microenvironment of PAC.

Key words: cancer cell-derived exosomes; miR-34a; SOCS3; tumor-associated macrophages; M1/M2 polarization.

Correspondence: Wenzhi Dong, Department of Three Wards of Hepatobiliary Surgery, The Second Affiliated Hospital of Kunming Medical University, No. 374 Dianmian Road, Kunming, Yunnan 650101, China.
E-mail: dongwenzhi@kmmu.edu.cn

Contributions: WD, study concept and design, manuscript revision for important intellectual content, funding acquisition; QZ, literature search, data extraction; XK, statistical processing and analysis of data interpretation; KL, manuscript original drafting, and revision for intellectual content. All the authors read and approved the final version of the manuscript and agreed to be accountable for all aspects of the work.

Conflict of interest: the authors declare no competing interest, and all authors confirm accuracy.

Ethics approval: experimental protocols were approved by the Ethics Committee of the Second Affiliated Hospital of Kunming Medical University (approval no. kmmu20220404). Written informed consent was obtained from the participants in the study.

Availability of data: data is not publicly available due to ethical reasons. Data will be made available on reasonable requests to the corresponding author.

Funding: this work was supported by the Science and Technology Planning project of Yunnan Science and Technology Department (202001AY070001-220).

Introduction

Pancreatic cancer (PAC) is a highly malignant gastrointestinal tumor with morbidity almost equal to mortality and is the seventh major cause of cancer-related deaths worldwide.[1] Based on the most recent global cancer statistics, approximately 470,000 deaths from PAC occurred worldwide in 2020.[2] The surgical resection ratio of PAC is relatively low owing to tumor metastasis and peripheral vascular infiltration, and the recurrence rate is high. In addition, the prognosis for patients with PAC is unfavorable, and the 5-year survival rate is merely 9%; tumor invasion and metastasis act as the leading causes of poor prognosis in patients suffering from PAC.[3] However, the mechanisms of the invasion and metastasis of PAC have not been fully understood. Therefore, further illumination of the molecular mechanisms of PAC invasion and metastasis and identification of more effective targets for intervention are of great significance for treating PAC and prolonging patient survival.

The tumor microenvironment (TME) is a complex environment for tumor growth, and macrophages are the most infiltrated immune cells around tumor tissues, also known as tumor-associated macrophages (TAMs).[4] TAMs play a crucial regulatory role in the TME by mediating immunosuppression and promoting angiogenesis and tumor metastasis.[5] The phenotype and function of TAMs are closely related to the TME. TAMs can be induced into M1 and M2 polarization phenotypes. Macrophages with M1 phenotype secrete interleukin (IL)-6, IL-12, inducible tumor necrosis factor-alpha, nitric oxide synthase, and IL-1β, promoting inflammatory responses and exerting antitumor effects. Macrophages with M2 phenotype mainly secrete arginase 1, transforming growth factor-beta (TGF-β) cytokines, and IL-10, promoting tumor development and immunosuppression.[6] Studies have shown that TAMs are mostly M2-polarized macrophages and that the transformation of TAMs from the M1 to M2 phenotype is an essential event in tumor progression.[7] Therefore, blocking the function of TAMs in the TME may be a potential therapeutic strategy for inhibiting tumor development, such as inhibiting the differentiation of TAMs, blocking TAM activation, and reprogramming TAMs into the M1 phenotype.[8] However, the molecular mechanisms that regulate the transformation of different TAM phenotypes are not fully understood. Thus, understanding the regulatory mechanisms underlying M2 polarization in PAC may offer new therapeutic opportunities for targeting TAMs to inhibit tumor progression.

Extracellular vesicles (EVs) represent a general term for diverse vesicles with membrane structures emitted by cells.[9] According to the classification of EVs by the International Society of Extracellular Vesicles, exosomes are EVs with a double-layer vesicle structure with a diameter of 30-150 nm.[10] Studies have found that exosomes carry a series of bioactive substances, including miRNA, mRNA, protein, and lipids.[11] These exosomal components act as molecular mediators in intercellular communication within the TME, influencing tumor progression through multiple mechanisms, including immune modulation and metastasis promotion.[12] In addition, exosomes have been explored as potential drug delivery systems.[13-15] Fang *et al.*[16] demonstrated that exosomal miR-1247-3p from highly metastatic hepatocellular carcinoma (HCC) cells activates tumor-associated fibroblasts by targeting beta-1,4-galactosyltransferase 3, thereby promoting lung metastasis of HCC. Additionally, tumor-derived exosomes have been implicated in regulating macrophage polarization, influencing the immunosuppressive properties of the TME and thereby affecting tumor progression.[17] For instance, the exosomal miR-934 originating from tumors induces M2 polarization, which in turn promotes metastasis by regulating the interaction between colorectal cancer cells and TAMs.[18] Wang *et al.*[19] discovered that hypoxic exosomes originated from PAC cells activate macrophages into the M2 phenotype in a hypoxia-inducible factor 1α or 2α-dependent manner and facilitate PAC cell epithelial-mesenchymal transition (EMT), migration, and invasion. Previous studies have demonstrated that miR-221 reduces the proliferation of the human PAC cells PANC-1[20] by inhibiting SOCS3 and affecting the Janus kinase-signal transducers and activators of transcription 3 (JAK-STAT3) signaling pathway. SOCS3 plays an essential role in PAC development. However, whether miR-34a regulates PAC progression by targeting SOCS3, specifically, whether exosomal miR-34a can modulate the transition of TAMs toward the M2 phenotype and subsequently affect the malignancy of PAC cells requires further investigation.

In this study, we explored the role of miR-34a in PAC cell-derived exosomes and its effect on TAM polarization. We hypothesized that exosomal miR-34a could suppress the malignant progression of PAC by reprogramming TAMs toward an antitumor phenotype through targeting suppressor of cytokine signaling 3 (SOCS3), a known regulator of the JAK-STAT pathway. Our findings provide new insights into the regulatory mechanisms underlying PAC progression and suggest potential therapeutic strategies for targeting the TME in PAC.

Materials and Methods

Clinical specimens

Twenty patients with PAC, including 13 men and 7 women, who underwent surgery at the Second Affiliated Hospital of Kunming Medical University from May 2020 to May 2021, were selected. The patients were 35-67 years old with a median age of 48. No patient received chemotherapy or radiotherapy before the operation. Fresh and normal tumor tissue samples were collected. All patients provided informed consent. This study was evaluated and sanctioned by the Ethics Committee of the Second Affiliated Hospital of Kunming Medical University. The association of miR-34a levels and the clinicopathological characteristics of patients suffering from PAC is displayed in Table 1.

Cell culture and the induction of macrophages

The cell lines HPDE6-c7, PANC-1, HPAF-II, MIA PaCa-2, THP-1, and SW1990 used in the study were acquired from the ATCC. ATCC performs quality control specifications including Mycoplasma contamination testing, population doubling capacity, population doubling time, and short tandem repeat (STR) profiling for all cell lines. Cell lines were passaged for less than 6 months after receipt and resuscitation, and no reauthentication was performed within this period. HPAF-II cells were cultivated in MEM, RPMI-1640 medium supported the growth of THP-1 cells, and all the other cells were maintained in DMEM.

To the medium, 10% fetal bovine serum and 1% 100× penicillin-streptomycin solution were added. The cells were cultivated in the cell incubator (SANYO, Japan) containing 95% air and 5% CO_2 at 37°C. The reagents utilized for cell culture were bought from Gibco (USA).

Induction of macrophages: THP-1 cells were inoculated into the plate, and phorbol 12-myristate 13-acetate(PMA) solution was added to a final concentration of 200 nM/L. PMA is a potent activator of protein kinase C (PKC), which is commonly used to differentiate monocytes into macrophages. After 48 h, the cells adhered to the wall and extended their pseudopodia, indicating the successful induction of M0 macrophages.

Cell transfection

A 6-well plate received an inoculation of cells (1×10^6), cultured overnight, and transfected when confluence reached 80%. Lipofectamine 2000 (Invitrogen, Waltham, MA, USA) and miR-NC mimics/miR-34a mimics were mixed with 250 µL of Opti-MEM (Gibco, Waltham, MA, USA) and incubated for 5 min. They were gently mixed and incubated for 30 min. The mixture was added to the wells, transfected for 4 h, and then replaced with normal medium. Cells were grown in culture for 24 h prior for subsequent experiments. The miRNA mimics were synthesized by RioBio Co., Ltd. (Guangzhou, China).

In situ hybridization

Digoxin *in situ* hybridization (ISH) kit was purchased from Bersinbio Co., Ltd. (Guangzhou, China). Clinical tissue samples were fixed in 4% paraformaldehyde at 4°C for 24 h, followed by dehydration, paraffin embedding, and sectioning at a thickness of 4 µm. Paraffin-embedded sections underwent deparaffinization in xylene (twice for 10 min each), rehydration in descending ethanol series (100%, 95%, 85%, 75%, and 50%), and endogenous peroxidase inactivation using 3% hydrogen peroxide at room temperature for 10 min.

For ISH to detect miR-34a, hybridization was performed using the specific probe following the manufacturer's instructions. The sections were incubated with the probe at 37°C overnight in a humidified chamber. Post-hybridization washes were carried out with SSC buffer (2×SSC at 37°C for 5 min, followed by 1×SSC and 0.5×SSC at 37°C for 10 min each). After hybridization, the sections were dehydrated in graded ethanol, air-dried, counterstained with Nuclear Fast Red, and observed under a microscope.

Positivity for ISH was assessed based on the presence of distinct brown signals in the cytoplasm, indicating miR-34a expression. Multiple fields per sample were observed and images were captured using a Nikon (Tokyo, Japan) microscope equipped with 10× and 40× objectives.

RT-qPCR

The extraction of total RNA from 1×10^6 cells was performed with the TRIzol kit (Absin Bioscience, Inc., Shanghai, China). The process of reverse transcription utilized PrimeScript RT Master Mix (Takara Biomedical Technology Co., Ltd., Beijing, China) following the manufacturer's instructions. All primers were synthesized by Takara, and the sequences can be found in Table 2. Then, qPCR was performed according to the instructions of the TB

Table 1. Association of miR-34a expression with clinicopathological features of patients with pancreatic cancer.

Clinical features	n	miR-34a expression, n		*p*
		High	Low	
Age (yrs)				0.6646
11	6	7		
≥48	9	5	4	
Gender				0.0072*
Male	13	3	10	
Female	7	6	1	
Tobacco smoke				0.0679
Yes	8	2	6	
No	12	8	4	
Lymph node metastasis				0.1421
Yes	12	7	5	
No	8	2	6	
Tumor size (cm)				0.0096*
6	5	1		
≥4	14	3	11	
TNM stage				0.0022*
I-II	7	6	1	
III-IV	13	2	11	
Distant metastasis				0.0608
Yes	16	12	4	
No	4	1	3	

*$p<0.001$.

Table 2. Primer sequences required for RT-qPCR.

Gene	Forward (5′-3′)	Reverse (5′-3′)
miR-34a	UGGCAGUGUCUUAGCUGGUUGU	AACCAGCUAAGACACUGCCAUU
ARG-1	ACTGACAACCACAAGTGGA	GCACATCGGGAATCTTTCC
CD206	ATGACCTTCAGTATCACAACCT	CTTCGTGATTTCATCTTGCAG
iNOS	ATGACCTTCAGTATCACAACCT	CTGGAGACTTCTTTCCCGT
CD86	AGTGCTTGCTAACTTCAGTC	CGTGTATAGATGAGCAGGTC
SOCS3	GTTCCACCTCGAGCTCTCC	CCTCGGAGGAGGGTTCAGTA
U6	CTCGCTTCGGCAGCACA	AACGCTTCACGAATTTGCGT
β-actin	GAAGATCAAGATCATTGCTCCTC	ATCCACATCTGCTGGAAGG

Green® Fast qPCR Mix kit (Takara Biomedical Technology). U6 snRNA and β-actin were used as internal references for miR-34a and mRNAs. The relative expression levels of genes were analyzed by means of the $2^{-\Delta\Delta Ct}$ method. The experiment was carried out three times, and the results were averaged.

CCK-8 assay

Cells with a concentration of 4×10^4 mL were sown in a 96-well plate with each well containing 100 µL and cultivated for 24 h. Then, 10 µL of CCK-8 reagent (Sigma-Aldrich, St. Louis, MO, USA) was added to each well and incubated for 2 h. The absorbance was determined at 450 nm with a microplate reader (Epoch2, Agilent, Santa Clara, CA, USA). Each sample was analyzed three times in triplicate, and three repetitions of the experiment were performed.

Wound-healing assay

Cells were seeded at a density of 5×10^5 cells per well in a 6-well plate and cultured overnight until a confluent monolayer was formed. A scratch was then created using a sterile pipette tip. After washing with PBS five times, the medium was added, and the migration of cells at 0 h was photographed using a Nikon microscope equipped with a 10× objective. Each condition was assessed in triplicate. The cells were then cultured, and pictures were taken after 48 h. The scratch distance between two images was employed to measure the migratory capacity of the cells.

Transwell assay

Matrigel (Corning, Inc., Corning, NY, USA) was thawed on ice and mixed with RPMI-1640 medium at a ratio of 1:4. Then, 50 µL of diluted Matrigel was added to one-half of the upper chambers of the Transwell and incubated overnight to make it solidify. The cell suspension was adjusted to a density 5×10^4 cells/ mL. For the invasion assay, 100 µL of cell suspension was seeded into the upper chamber of Transwell (Corning), while 500 µL of medium was placed in the lower chamber. After culturing for 48 h, the medium was discarded, and the cells were treated with paraformaldehyde (TCI Development Co., Ltd., Shanghai, China) for fixation and subsequently stained using crystal violet (TCI Development Co., Ltd.). For the migration assay, the procedures were the same as those for the invasion assay, except that Matrigel did not need to be coated on the upper chamber of the Transwell. Cell migration and invasion were observed and recorded using a Nikon microscope equipped with a 10× objective. Each condition was assessed in triplicate.

Extraction and identification of exosomes

The supernatant of the cell culture was gathered and then centrifuged at 4°C for 10 min at 500 × g and 20 min at 12,000 × *g*. After the supernatant was filtered using a 0.22-µm filter, it was centrifuged at 100,000 × g for 2 h, and the centrifugation was repeated once. The pellet was resuspended in PBS for use. To identify exosomes, they were resuspended in PBS containing 2% paraformaldehyde, and 10 µL of the exosomes were dropped onto the copper mesh and dried at room temperature (RT) for 30 min. The exosomes on the copper mesh were stained with 2% phosphotungstic acid (Macklin Biochemical Co., Ltd., Shanghai, China) at RT for 2 min. Transmission electron microscopy (JEM-1400, Japan) was used to observe and record the exosomes. A nanoparticle analyzer (Nanosight LM10, Malvern Panalytical, Malvern, UK) employing tracking analysis was used to measure the exosome particle size. Three groups of exosomes were used in this study: PANC-1-Exo (Panc-1-exomir-34a mimic), PANC-1-Exo$^{miR\text{-}34a\ mimic}$ (exosomes extracted from PANC-1 cells transfected with miR-34a mimic), and PANC-1-Exo$^{NC\ mimic}$ (exosomes derived from mimic PANC-1 cells transfected with NC).

Western blot analysis

Exosomes and cells were lysed using the protein lysis buffer (Beyotime, Jangsu, China) on ice (20 min), and centrifuged at 12,000 × g, 4°C (20 min), and the supernatant was reserved. The protein concentration was determined with a BCA kit (Beyotime). Sodium dodecyl-sulfate-polyacrylamide gel electrophoresis and transfer were performed as previously described.[21] The polyvinylidene fluoride (PVDF) membrane (Millipore, Burlington, MA, USA) was blocked and then incubated with primary antibodies at 4°C throughout the night. The following day, the PVDF membrane was rinsed and incubated with secondary antibodies at RT for 1 h. At last, the PVDF membrane was processed with an ECL reagent (Invitrogen) and analyzed *via* a gel imaging system (ChemiDoc XRS, Bio-Rad Laboratories, Inc., Hercules, CA, USA). Antibodies were obtained from Abcam (Cambridge, UK), including anti-TSG101 (ab125011, 1:5,000), anti-CD63 (ab271286, 1:10,000), anti-E-cadherin (ab40772, 1:30,000), anti-N-cadherin (ab18203, 1:5,000), anti-vimentin (ab137321, 1:1,000), anti-β-actin (ab8226, 1:10,000), anti-SOCS3(ab280884, 1:1,000), anti-JAK1 (ab125051, 1:10,000), anti-JAK1 (phospho Y1022 + Y1023) (ab138005, 1:5,000), anti-STAT1 (ab210524, 1:1,000), anti-STAT1 (phospho S727) (ab109461, 1:5,000), goat anti-mouse IgG (ab6708, 1:10,000), and goat anti-rabbit IgG (ab6702, 1:5,000).

Exosome tracking

The exosome membrane was labeled with PKH26 (Umibio Biotechnology Co., Ltd., Shanghai, China). Then, 50 µL of 100 µM PKH26 solution was added to 100 µg of exosomes. After incubation for 10 min in the dark, 10 mL of PBS was added and mixed. The exosomes were extracted again by centrifugation to remove the excess dye. The pellet was co-incubated with induced M0 macrophages for 4 h. Macrophages were seeded onto glass coverslips placed in 24-well plates and allowed to adhere overnight before exosome treatment. For fixation, macrophages were immersed in 4% paraformaldehyde for a duration of 10 min. After rinsing, the slides were enclosed with an antifade mounting medium containing DAPI (Beyotime), were observed, and were photographed using a laser scanning confocal microscope (TCS SP5; Leica, Tokyo, Japan) with a 63x oil immersion objective.

Coculture experiment of macrophages and PANC-1 cells

Macrophages derived from induced THP 1 were implanted into the upper chamber of the Transwell. Macrophages were not seeded in the blank group. PANC-1+M/Exo$^{NC\ mimic}$ and PANC-1+M/Exo$^{miR\text{-}34a\ mimic}$ groups were added to the corresponding PANC-1-derived exosomes. After 48 h, the medium was changed, and PANC-1 cells were cultured in the lower chamber. After 48 h, PANC-1 cells were collected for subsequent experiments.

ELISA

The levels of cytokines secreted by the macrophages were detected using ELISA kits (Beyotime). Briefly, the gradient-diluted standard and cell culture supernatant were added to the wells and incubated at 37°C for 90 min. Then, the captured IL-10 or TGFβ was sequentially labeled with biotinylated antibodies and horseradish peroxidase-labeled streptavidin. Subsequently, the developer TMB solution was added and incubated at RT for 20 min in the dark. Finally, precisely 50 µL/well of the stop solution was carefully added in a meticulous manner. Subsequently, after thorough and uniform mixing, the absorbance at 450 nm was promptly and accurately measured using a highly calibrated and sensitive spectrophotometer.

Dual luciferase reporter gene assay

The nucleotide sequence of SOCS3 containing the miR-34a binding site was amplified using PCR. In addition, the binding site was subjected to point mutations, and the wild-type (WT) or mutant (MUT) nucleotide sequence of SOCS3 was cloned into the pmirGLO vector (BioVector NTCC Inc., Guangzhou, China) to construct luciferase, WT-SOCS3, and MUT-SOCS3 vectors. These processes were performed by GenePharma (Shanghai, China). Macrophages were planted in a 6-well plate and co-transfected with WT-SOCS3 and miR-34a mimic or miR-NC, MUT-SOCS3 and miR-34a mimic, or miR-NC. After 24 h, the activity of luciferase was detected with a dual-luciferase activity detection kit (Promega, Madison, WI, USA).

Statistical analysis

Statistical analysis was conducted using SPSS V22.0 software, and the data are presented as mean ± SD. Before performing statistical analysis, data normality was assessed using the Shapiro-Wilk test, and homogeneity of variance was examined using Levene's test. For comparisons between two groups, an independent sample *t*-test was used. For comparisons among multiple groups, one-way analysis of variance (ANOVA) was applied, followed by Tukey's honest significant difference (HSD) test for post hoc multiple comparisons when the variance was homogeneous. A *p*-value of less than 0.05 ($p<0.05$) signifies a statistically significant difference.

Results

miR-34a has a low expression in PAC

To assess the levels of miR-34a in PAC, we measured miR-34a in clinical tissues and PAC cell lines. In clinical tissues, miR-34a expression was significantly lower compared to nearby normal tissues and was primarily found in the cytoplasm. (Figure 1A). Furthermore, the levels of miR-34a in four PAC cell lines, PANC-1, W1990, HPAF-II, and MIA PaCa-2, were also lower than those in the human normal pancreatic ductal epithelial cell line HPDE6-C7, among which the relative level of miR-34a in PANC-1 cells was the lowest (Figure 1B); therefore, we used PANC-1 cells for subsequent experiments.

Overexpression of miR-34a inhibits the proliferation, migration, and invasion of PAC cells

To explore the role of miR-34a in PAC progression, miR-34a was overexpressed in PANC-1 cells, and the transfection efficiency was validated using RT-qPCR. (Figure 2A). We noticed that excessive expression of miR-34a not only reduced the viability of PANC-1 cells (Figure 2B) but also accelerated their apoptosis (Figure 2C). In addition, the rate of cell proliferation and migration in the miR-34a mimic group was lower than that in the miR-NC mimic group 48 h after scratching the cell culture dish (Figure 3A). The Transwell assay showed that the miR-34a mimic group had a reduced number of cells in the lower chamber compared to the

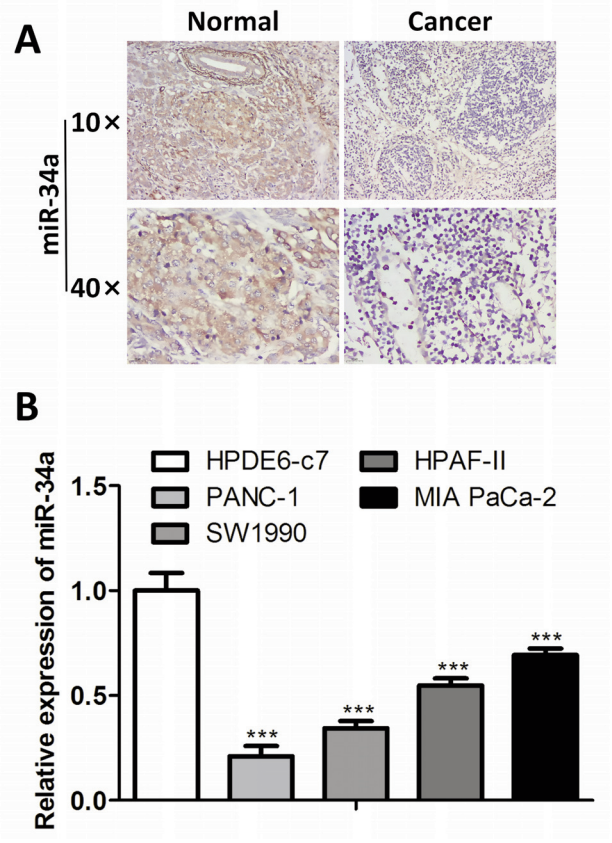

Figure 1. The level of miR-34a in PCA clinical tissues and cell lines. **A**) The expression of miR-34a in clinical samples was detected using ISH; scale bar: 100 μm. **B**) The expression of miR-34a in PANC-1, W1990, HPAF-II, MIA PaCa-2, and HPDE6-C7 cells was detected using RT-qPCR; ***$p<0.001$.

miR-NC mimic group (Figure 3B). These results suggest that the overexpression of miR-34a inhibits the proliferation, migration, and invasion of PAC cells.

miR-34a in PAC-derived exosomes inhibits M2 polarization of macrophages

Next, we studied the effect of miR-34a on TAM polarization in PAC-derived exosomes. First, exosomes secreted byPANC-1 and HPDE6-C7 cells were extracted and characterized with the use of transmission electron microscopy and nanoparticle tracking analysis. There was no difference in the morphology and particle size between the two groups of exosomes (Figure 4 A,B). Besides, the expression of the exosomal markers TSG101 and CD63 was verified (Figure 4C). Furthermore, we determined the content of miR-34a in exosomes and observed a decreased level of miR-34a in PANC-1-Exo (Figure 4D). However, the miR-34a level in exosomes derived from PANC-1 cells overexpressing miR-34a was higher than that in exosomes derived from the NC mimic group (Figure 4E). Subsequently, PANC-1-Exo was co-incubated with the induced M0 macrophages, PANC-1-Exo was phagocytosed entirely by macrophages (Figure 4F). In addition, the high miR-34a level were detected in macrophages that phagocytosed the PANC-1-Exo$^{miR\text{-}34a\ mimic}$ (Figure 4G). After the PANC-1-Exo$^{miR\text{-}34a\ mimic}$ was phagocytosed, the expression levels of the M2 polarization markers arginase 1 and CD206 were lower than those in the PANC-1-Exo$^{NC\ mimic}$ and IL-4-stimulated groups. The expression levels of inducible nitric oxide synthase and CD86, markers of M1 polarization, were consistent in each group (Figure 5A). The ELISA detection results of IL10 and TGFβ, which are the cytokine markers of M2 polarization in the cell culture supernatant, also showed that miR-34a in PAC-derived exosomes inhibit M2 polarization of macrophages (Figure 5B).

miR-34a in PAC-derived exosomes inhibits migration, invasion, and EMT by inhibiting M2 polarization of macrophages

To further study the effect of miR-34a in PAC-derived exosomes on tumor progression after inhibiting the M2 polarization of macrophages, we co-incubated PANC-1 cells with the exosome-free supernatant of macrophages treated with exosomes (Figure 6A). Next, the invasion and migration abilities of the PANC-1 cells were evaluated. In comparison to the groups treated with control and M0 macrophage supernatant, the migration and invasion ability of PANC-1 cells were enhanced after co-incubated with the supernatant of macrophages treated with PANC-1-Exo$^{NC\ mimic}$. After co-incubation with the supernatant of macrophages treated with the PANC-1-Exo$^{miR\text{-}34a\ mimic}$, the invasion and migration abilities of PANC-1 cells were weakened compared with those of the M/Exo$^{NC\ mimic}$ group (Figure 6B). In addition, we investigated the levels of EMT-related proteins, including vimentin, N-cadherin, and E-cadherin, in PANC-1 cells. The results indicated that, in comparison with the M/Exo$^{NC\ mimic}$ group, the expression of E-cadherin was elevated, while the expression of N-cadherin and vimentin was reduced in the M/Exo$^{miR\text{-}34a\ mimic}$ group (Figure 6C). These results suggest that miR-34a in PAC-derived exosomes inhibits the EMT of PAC by inhibiting M2 polarization of macrophages.

SOCS3 is directly targeted by miR-34a

To identify the direct target of miR-34a, the TargetScan database (version 7.2) was used for prediction and screening, and SOCS3 was identified as a potential target of miR-34a. Information on the binding sites of the two proteins is shown in Figure 7A. By establishing a dual-luciferase reporter plasmid and transfecting it into macrophages, it was determined that SOCS3

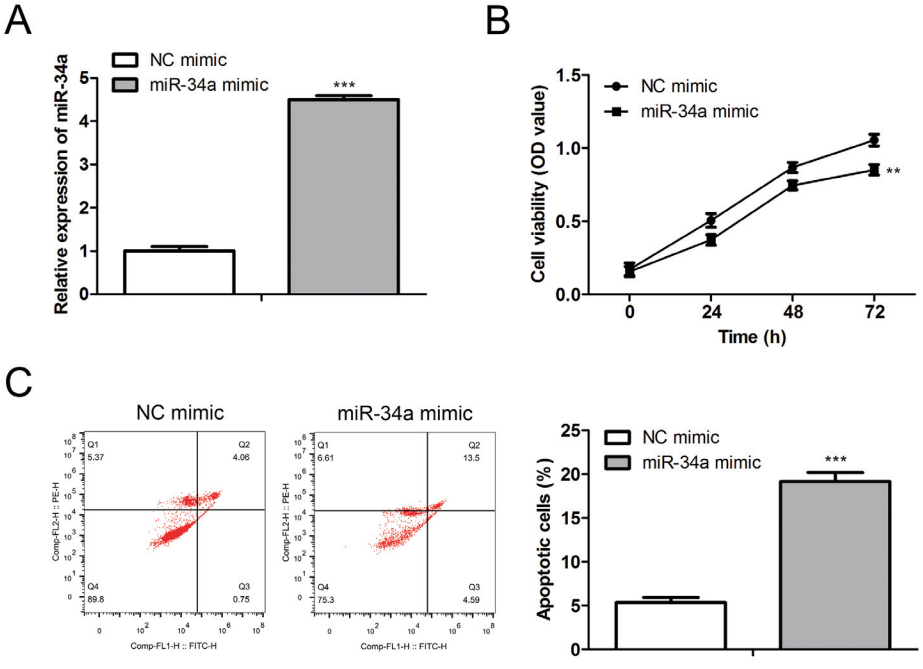

Figure 2. The effect of miR-34a on the proliferation and apoptosis of PANC-1. **A**) The transfection efficiency of miR-34a was evaluated using RT-qPCR; ***p<0.001. **B**) Cell proliferation was detected using the CCK-8 assay; **p<0.01. **C**) Cell apoptosis was detected using flow cytometry; ***p<0.001.

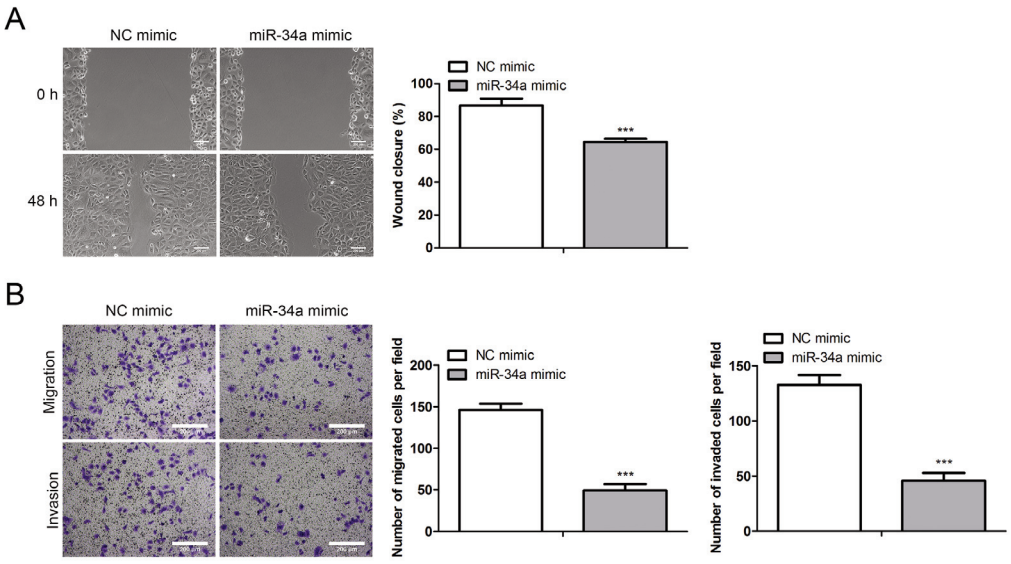

Figure 3. The effect of miR-34a on the migration and invasion of PANC-1. **A**) A wound-healing assay was used to assess cell migration ability; scale bar: 200 μm; ***p<0.001. **B**) Transwell assay was performed to assess cell migration and invasion; scale bar: 200 μm; ***p<0.001.

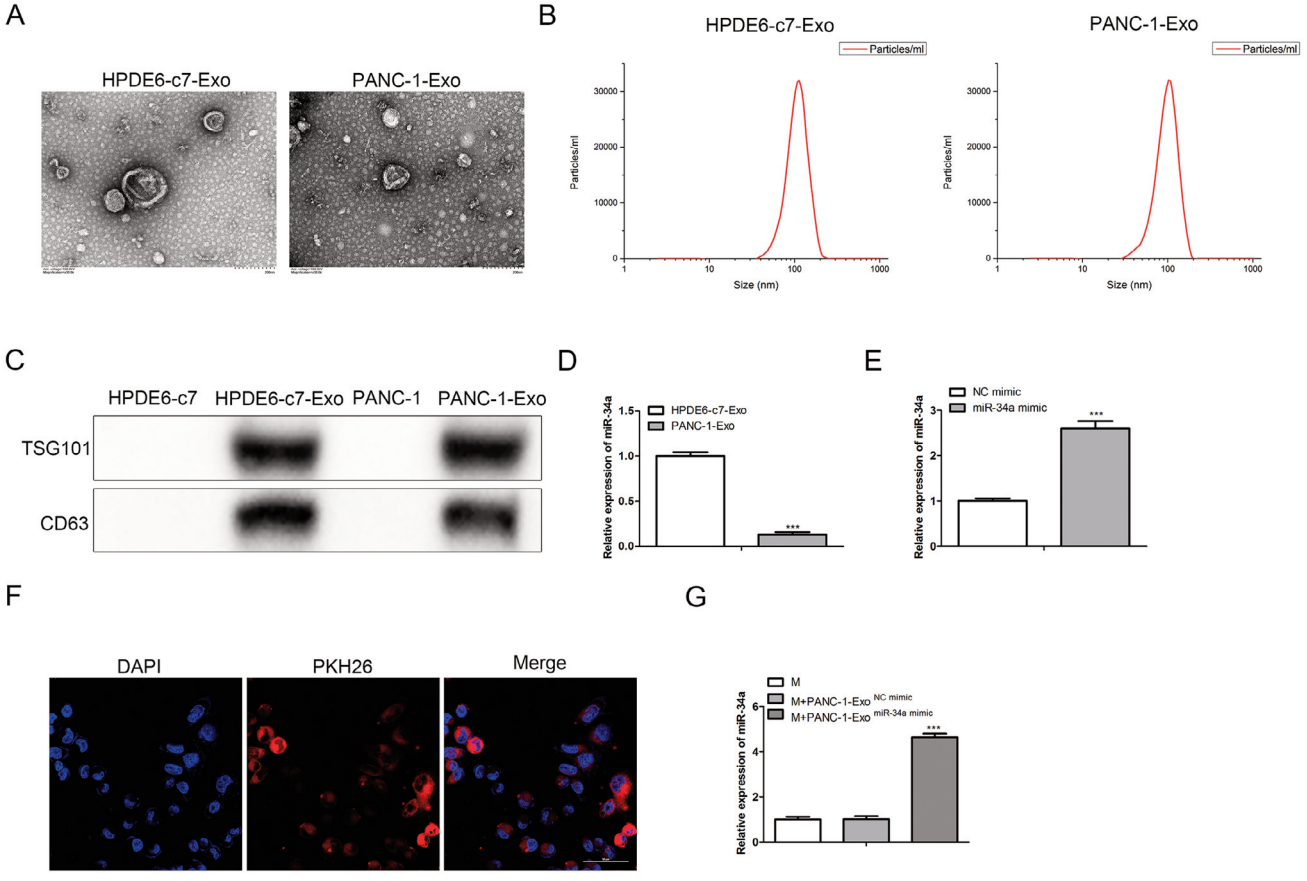

Figure 4. MiR-34a is phagocytosed into macrophages through cancer cell-derived exosomes. **A**) TEM images of exosomes derived from HPDE6-C7 and PANC-1 cells. **B**) NTA of the two exosome types. **C**) Exosome markers were detected by western blotting. **D**) Expression of miR-34a in exosomes derived from HPDE6-C7 and PANC-1 cells was evaluated using RT-qPCR; ***p<0.001. **E**) Expression of miR-34a in miR-34a-overexpressed PANC-1-derived exosomes; ***p<0.001. **F**) Exosome tracing by PKH26 labeling; scale bar: 200 μm. **G**) The expression of miR-34a in macrophages, macrophages+ PANC-1-Exo$^{NC\ mimic}$, and macrophages+ PANC-1-Exo$^{miR\text{-}34a\ mimic}$; ***p<0.001.

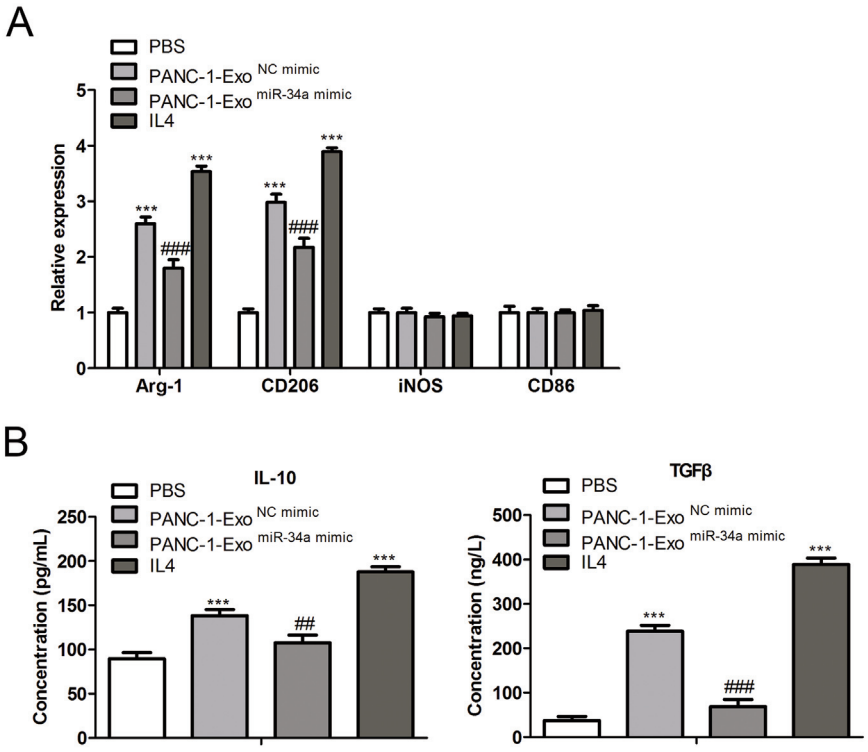

Figure 5. Exosomal miR-34a inhibits M2 polarization of macrophages. **A**) The expression of M1/M2 polarization markers in macrophages treated with PBS, PANC-1-Exo$^{NC\ mimic}$, PANC-1-$^{ExomiR-34a\ mimic}$, and IL-4 was evaluated using RT-qPCR; ***p<0.001 *vs* PBS group, $^{###}p$<0.001 vs PANC-1-Exo$^{NC\ mimic}$ group. **B**) Secretion of M2 polarization marker cytokines in the four groups was detected using ELISA; ***p<0.001 *vs* PBS group, $^{###}p$<0.001 *vs* PANC-1-Exo$^{NC\ mimic}$ group.

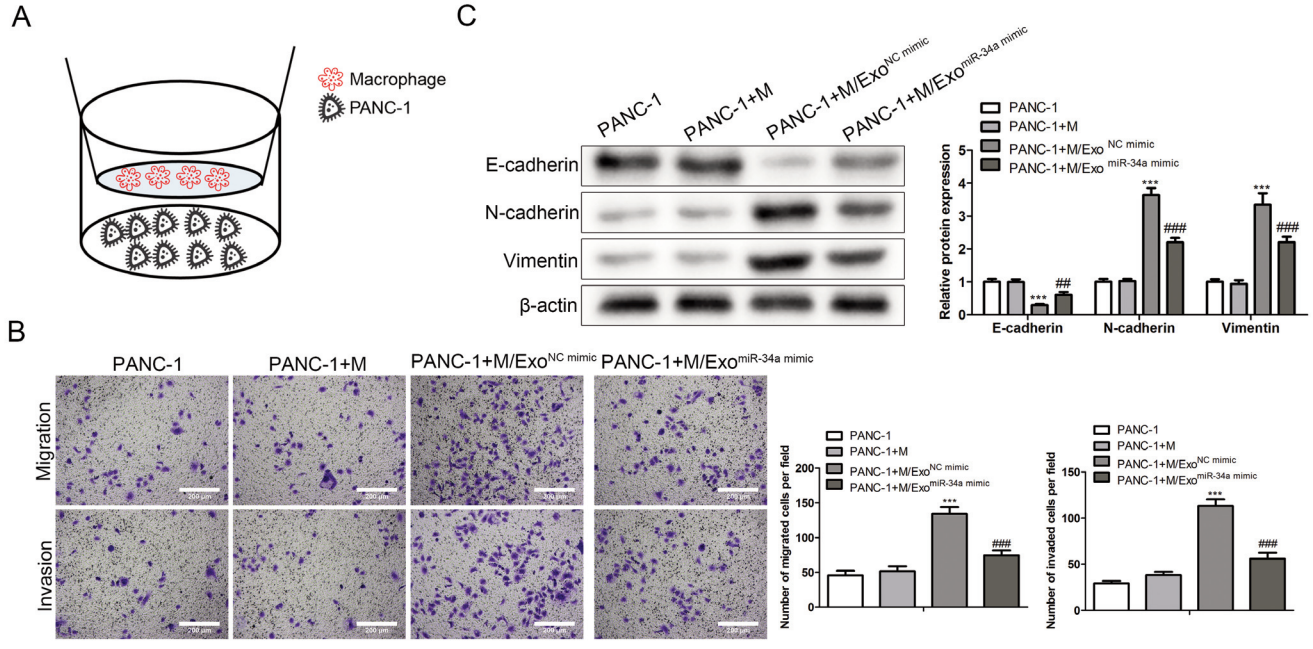

Figure 6. Exosomal miR-34a inhibits the migration, invasion, and EMT of PANC-1 cells by suppressing the M2 polarization of macrophages. **A**) Schematic diagram of the coculture of PANC-1 cells and macrophages. **B**) Migration and invasion of PANC-1 cells were evaluated by Transwell assay after coculture with exosome-treated macrophages; scale bar: 200 μm; ***p<0.001 *vs* PANC-1+M group, $^{###}p$<0.001 *vs* PANC-1+M/$^{ExoNC\ mimic}$ group. **C**) EMT-related proteins were detected using Western blotting; ***p<0.001 *vs* PANC-1+M group, $^{###}p$<0.001 *vs* PANC-1+M/$^{ExoNC\ mimic}$ group.

was a direct target of miR-34a (Figure 7B). After transfection of macrophages with the miR-34a mimic, SOCS3 expression was downregulated (Figure 7C). Macrophages were then treated with PANC-1-derived Exo$^{miR\text{-}34a\ mimic}$ and Exo$^{NC\ mimic}$. The expression of SOCS3 was downregulated in macrophages treated with the Exo$^{miR\text{-}34a\ mimic}$, and the expression of JAK1 and STAT1 did not change significantly; however, the expression of their phosphorylated proteins was upregulated (Figure 7D). This suggests that miR-34a inhibits M2 macrophage polarization by regulating the SOCS3/JAK/STAT1 pathway.

miR-34a/SOCS3 axis affects PAC malignant progression by regulating M2 polarization of macrophage

Next, we explored whether the regulation of the miR-34a/SOCS3 axis on the M2 polarization of macrophages further affected the proliferation, invasion, and migration of PAC cells using a rescue assay. To this end, SOCS3 or NC was overexpressed in macrophages, which were treated with Exo$^{miR\text{-}34a\ mimic}$ or Exo$^{NC\ mimic}$, and the supernatant of macrophages was co-incubated with PANC-1 cells. PANC-1 cells showed the highest cell viability after co-incubation with the M-pc-NC/Exo$^{NC\ mimic}$ and decreased cell viability after co-incubation with the M-pc-NC/Exo$^{miR\text{-}34a\ mimic}$. However, after overexpression of SOCS3 in macrophages, cell viability increased again compared with the coculture with the M-pc-NC/Exo$^{miR\text{-}34a\ mimic}$ (*Supplementary Figure S1A*). A similar trend was witnessed in the Transwell migration. and invasion assays (Supplementary Figure S1B). These outcomes verified the negative regulatory connection between miR-34a and SOCS3 and confirmed that the miR-34a /SOCS3 axis suppresses the malignant progression of PAC cells by inhibiting the M2 polarization of macrophages.

Discussion

Macrophages are mainly polarized into M2-type TAMs in the TME, which play essential roles in tumor growth, proliferation, metastasis, and invasion.[22] Research has indicated that miRNAs play a vital role in regulating the polarization of macrophages into TAMs.[23] MiR-145 regulates the polarization of TAMs by EVs secreted by colorectal cancer.[2]. MiR-34 family members are tumor suppressors induced by p53 transcription and are closely associated with human cancers.[25] Downregulation of miR-34 family members is considered a critical factor in the development of ovarian cancer.[26] Li *et al.*[27] found that tumor-associated fibroblasts promote cancer cell proliferation and metastasis through exosome-mediated paracrine miR-34a-5p in oral cancer. Tang *et al*.[28] also reported that miR-34a inhibits PAC progression by targeting Snail1-mediated EMT and Notch pathways. MiR-34a has also been shown to inhibit the polarization of M1 macrophages during osteolysis.[29] Exosomal miR-34a secreted by adipocytes promotes adipose inflammation by inhibiting the polarization of M2 macrophages.[30] In addition, exosome-coated miR-34a showed potent antitumor activity against PAC, both *in vitro* and *in vivo*.[31] However, the effects of miR-34a on the polarization of TAMs and the related mechanisms have not been reported. This study found that miR-34a was highly expressed in PAC-derived exosomes. To explore the role of exosomal miR-34a in macrophage polarization, we used phorbol 12-myristate 13-acetate to induce monocyte THP-1 cells to construct a macrophage model and obtain M0-type macrophages. We found that PAC-derived exosomes polarized M0 macrophages into the M2 phenotype, while the miR-34a-overexpressed PAC-derived exosomes inhibited the transformation of M0 macrophages to the M2 phenotype. These findings suggest that exosomes originating from cancer cells activate the polarization of macrophages, and exosomal miR-34a inhibits the M2 polarization of macrophages but has no impact on macrophage M1 polarization (Figure 5A).

Moreover, in the present study, we discovered that the invasion, migration, and EMT process of PANC-1 cells was markedly inhibited by the supernatant of macrophages treated with exosomes derived from miR-34a-overexpressed PANC-1 cells. However, M0 macrophages that were not treated with exosomes did not affect the progression of PANC-1. This indicates that exosome-derived miR-34a can inhibit the malignant progression of PAC cells by inhibiting the M2 polarization of macrophages. Similarly, Liu *et al.*[32] also observed that miR-770 in exosomes from tumors hindered the advancement of non-small cell lung cancer by preventing macrophages from polarizing to the M2 type.

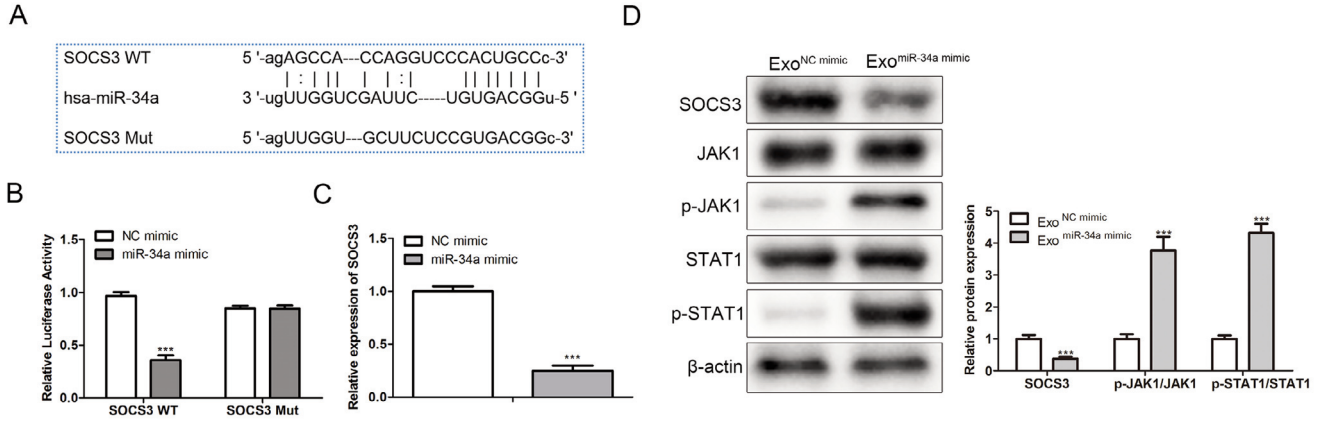

Figure 7. SOCS3 is the direct target of miR-34a. **A**) The binding sites of SOCS3 and miR-34a were predicted using the TargetScan software. **B**) Relationship between SOCS3 and miR-34a was verified using a dual-luciferase reporter assay; ***p<0.001. **C**) Expression of miR-34a in macrophages transfected with miR-34a mimic; ***p<0.001. **D**) Expression of SOCS3, JAK1/STAT1, and their phosphorylated proteins was detected using Western blotting; ***p<0.001.

These results confirmed that exosomes originating from tumor cells influence the genesis and development of tumors by regulating the polarization of TAMs.

Herein, SOCS3 has been verified as a direct target of miR-34a, which regulates the polarization of macrophages through the negative regulation of SOCS3, thus affecting the malignant process of PAC cells. SOCS3 can negatively regulate the expression of the JAK/STAT signal pathway by binding to the phosphorylation docking sites of JAK/cytokine receptors or STAT receptors and their downstream target genes, preventing malignant transformation and apoptosis inhibition of cells.[33,34] Ji *et al.* found that reducing the expression of SOCS3 in a rat model of intracerebral hemorrhage promoted M2 polarization of macrophages.[35] Liu *et al.* reported that the upregulation of miR-221-3p in exosomes derived from TAMs with M2 polarization inhibits the expression of SOCS3 and aggravates osteosarcoma growth and metastasis by activating the JAK2/STAT3 pathway.[36] In this study, we found that after macrophages were treated with the $Exo^{miR\text{-}34a\ mimic}$, the expression of SOCS3 decreased. Although the expression of JAK1 and STAT1 did not change, the expression of their phosphorylated proteins increased, indicating the activation of the JAK/STAT signaling pathway.[37] These findings suggest that miR-34a activates the JAK/STAT signaling pathway by negatively regulating SOCS3 expression, thus promoting M2 polarization of macrophages and affecting PAC progression.

However, the mechanism by which SOCS regulates JAK/STAT to inhibit tumor progression is not only the effect of M2 macrophages alone but also a complex process involving multiple mechanisms.[34,38] It has been reported that the mechanism by which SOCS regulates JAK/STAT to inhibit tumor progression is also dysregulated with cytokine receptors, Toll-like receptors, and hormone receptors signaling,[39-41] IL-6,[42] long non-coding RNAs,[43] TME,[42,44] insulin-like growth factor-I,[45] and immune checkpoint molecules.[46] Therefore, the mechanism by which SOCS regulates JAK/STAT participation in the progression of pancreatic adenocarcinoma should be further explored.

This study had some limitations. Twenty clinical samples were collected for this study, limiting our understanding of this disease. To compensate for this limitation, future studies ought to consider expanding the sample size to validate our results more comprehensively. Whether exosomal miR-34a derived from PAC cells be capable of inhibiting the growth and metastasis of PAC *in vivo* by inhibiting M2 polarization of macrophages has not been tested *in vivo*, nor has it been verified in other cell lines. In addition, miRNAs have some problems in clinical applications, such as a lack of specificity and difficult delivery, and their side effects, safety, efficacy, and feasibility still need to be verified in more clinical trials. We plan to conduct more in-depth studies in the foreseeable future.

This study substantiated that miR-34a activates the JAK/STAT signaling pathway by targeting SOCS3, regulating the M2 polarization of macrophages and affecting the EMT, proliferation, migration, and invasion of PANC-1 cells. These findings provide a basis for clinical target detection and targeted therapy of pancreatic adenocarcinoma. The basic principle of treatment is that the overexpression of miR-34a can inhibit M2 polarization of macrophages through the negative regulation of SOCS to activate the JAK/STAT pathway and inhibit the development of pancreatic adenocarcinoma. While this study focused on the overall effects of miR-34a, future studies should investigate specific downstream target genes and cytokines that could play a significant role in PAC metastasis. This discovery is of great value in revealing the molecular mechanisms of PAC and its treatment.

References

1. Wild CP, Weiderpass E, Stewart BW. World cancer report: cancer research for cancer prevention. Lyon, International Agency for Research on Cancer; 2020.
2. Jain T, Dudeja V. The war against pancreatic cancer in 2020 - advances on all fronts. Nat Rev Gastroenterol Hepatol 2021;18:99-100.
3. Khalaf N, El-Serag HB, Abrams HR, Thrift AP. Burden of pancreatic cancer: from epidemiology to practice. Clin Gastroenterol Hepatol 2021;19:876-84.
4. Vitale I, Manic G, Coussens LM, Kroemer G, Galluzzi L. Macrophages and metabolism in the tumor microenvironment. Cell Metab 2019;30:36-50.
5. Hinshaw DC, Shevde LA. The tumor microenvironment innately modulates cancer progression. Cancer Res 2019;79:4557-66.
6. Rhee I. Diverse macrophages polarization in tumor microenvironment. Arch Pharm Res 2016;39:1588-96.
7. Mantovani A, Sozzani S, Locati M, Allavena P, Sica A. Macrophage polarization: tumor-associated macrophages as a paradigm for polarized M2 mononuclear phagocytes. Trends Immunol 2002;23:549-55.
8. Pathria P, Louis TL, Varner JA. Targeting tumor-associated macrophages in cancer. Trends Immunol 2019;40:310-27.
9. El Andaloussi S, Mäger I, Breakefield XO, Wood MJ. Extracellular vesicles: biology and emerging therapeutic opportunities. Nat Rev Drug Discov 2013;12:347-57.
10. Royo F, Théry C, Falcón-Pérez JM, Nieuwland R, Witwer KW. Methods for separation and characterization of extracellular vesicles: results of a worldwide survey performed by the ISEV rigor and standardization subcommittee. Cells 2020;9:1955.
11. Kok VC, Yu CC. Cancer-derived exosomes: their role in cancer biology and biomarker development. Int J Nanomedicine 2020;15:8019-36.
12. Zhang L, Yu D. Exosomes in cancer development, metastasis, and immunity. Biochim Biophys Acta Rev Cancer 2019;1871:455-68.
13. Hsu MT, Wang YK, Tseng YJ. Exosomal proteins and lipids as potential biomarkers for lung cancer diagnosis, prognosis, and treatment. Cancers (Basel) 2022;14:732.
14. Rashid MH, Borin TF, Ara R, Alptekin A, Liu Y, Arbab AS. Generation of novel diagnostic and therapeutic exosomes to detect and deplete protumorigenic m2 macrophages. Adv Ther (Weinh) 2020;3:1900209.
15. Xunian Z, Kalluri R. Biology and therapeutic potential of mesenchymal stem cell-derived exosomes. Cancer Sci 2020;111:3100-10.
16. Fang T, Lv H, Lv G, Li T, Wang C, Han Q, et al. Tumor-derived exosomal miR-1247-3p induces cancer-associated fibroblast activation to foster lung metastasis of liver cancer. Nat Commun 2018;9:191.
17. Baig MS, Roy A, Rajpoot S, Liu D, Savai R, Banerjee S, et al. Tumor-derived exosomes in the regulation of macrophage polarization. Inflamm Res 2020;69:435-51.
18. Zhao S, Mi Y, Guan B, Zheng B, Wei P, Gu Y, et al. Tumor-derived exosomal miR-934 induces macrophage M2 polarization to promote liver metastasis of colorectal cancer. J Hematol Oncol 2020;13:156.
19. Wang X, Luo G, Zhang K, Cao J, Huang C, Jiang T, et al. Hypoxic tumor-derived exosomal miR-301a mediates M2 macrophage polarization via PTEN/PI3Kgamma to promote pancreatic cancer metastasis. Cancer Res 2018;78:4586-98.
20. Xie J, Wen JT, Xue XJ, Zhang KP, Wang XZ, Cheng HH. MiR-221 inhibits proliferation of pancreatic cancer cells via down

regulation of SOCS3. Eur Rev Med Pharmacol Sci 2018;22:1914-21.
21. Osada-Oka M, Shiota M, Izumi Y, Nishiyama M, Tanaka M, Yamaguchi T, et al. Macrophage-derived exosomes induce inflammatory factors in endothelial cells under hypertensive conditions. Hypertension Res 2017;40:353-60.
22. Pritchard A, Tousif S, Wang Y, Hough K, Khan S, Strenkowski J, et al. Lung tumor cell-derived exosomes promote M2 macrophage polarization. Cells 2020;9:1303.
23. Essandoh K, Li Y, Huo J, Fan GV. miRNA-mediated macrophage polarization and its potential role in the regulation of inflammatory response. Shock 2016;46:122-31.
24. Shinohara H, Kuranaga Y, Kumazaki M, Sugito N, Yoshikawa Y, Takai T, et al. Regulated polarization of tumor-associated macrophages by miR-145 via colorectal cancer-derived extracellular vesicles. J Immunol 2017;199:1505-15.
25. Zhang L, Liao Y, Tang L. MicroRNA-34 family: a potential tumor suppressor and therapeutic candidate in cancer. J Exp Clin Cancer Res 2019;38:53.
26. Welponer H, Tsibulak I, Wieser V, Degasper C, Shivalingaiah G, Wenzel S, et al. The miR-34 family and its clinical significance in ovarian cancer. J Cancer 2020;11:1446.
27. Li Y-Y, Tao Y-W, Gao S, Li P, Zheng J-M, Zhang S-E, et al. Cancer-associated fibroblasts contribute to oral cancer cells proliferation and metastasis via exosome-mediated paracrine miR-34a-5p. EBioMedicine 2018;36:209-20.
28. Tang Y, Tang Y, Cheng Y-S. miR-34a inhibits pancreatic cancer progression through Snail1-mediated epithelial–mesenchymal transition and the Notch signaling pathway. Sci Rep 2017;7:38232.
29. Gao XR, Ge J, Li WY, Zhou WC, Xu L, Geng D-K. miR−34a carried by adipocyte exosomes inhibits the polarization of M1 macrophages in mouse osteolysis model. J Biomed Mat Res Part A 2021;109:994-1003.
30. Pan Y, Hui X, Hoo RLC, Ye D, Chan CYC, Feng T, Wang y, et al. Adipocyte-secreted exosomal microRNA-34a inhibits M2 macrophage polarization to promote obesity-induced adipose inflammation. J Clin Invest 2019;129:834-49.
31. Zuo L, Tao H, Xu H, Li C, Qiao G, Guo M, Cao S, et al. Exosomes-coated miR-34a displays potent antitumor activity in pancreatic cancer both in vitro and in vivo. Drug Des Devel Ther 2020;14:3495-507.
32. Liu J, Luo R, Wang J, Luan X, Wu D, Chen H, Hou Q, et al. Tumor Cell-derived exosomal miR-770 inhibits M2 macrophage polarization via targeting MAP3K1 to inhibit the invasion of non-small cell lung cancer cells. Front Cell Dev Biol 2021;9:1409.
33. Liu ZK, Li C, Zhang RY, Wei D, Shang YK, Yong YL, Kong LM, et al. EYA2 suppresses the progression of hepatocellular carcinoma via SOCS3-mediated blockade of JAK/STAT signaling. Mol Cancer 2021;20:79.
34. Dai L, Li Z, Tao Y, Liang W, Hu W, Zhou S, Fu X, et al. Emerging roles of suppressor of cytokine signaling 3 in human cancers. Biomed Pharmacother 2021;144:112262.
35. Ji XC, Shi YJ, Zhang Y, Chang MZ, Zhao G. Reducing suppressors of cytokine signaling-3 (SOCS3) Expression promotes M2 macrophage polarization and functional recovery after intracerebral hemorrhage. Front Neurol 2020;11:586905.
36. Liu W, Long Q, Zhang W, Zeng D, Hu B, Liu S, Chen L. miRNA-221-3p derived from M2-polarized tumor-associated macrophage exosomes aggravates the growth and metastasis of osteosarcoma through SOCS3/JAK2/STAT3 axis. Aging (Albany NY) 2021;13:19760.
37. Xin P, Xu X, Deng C, Liu S, Wang Y, Zhou X, Ma H, et al. The role of JAK/STAT signaling pathway and its inhibitors in diseases. Int Immunopharmacol 2020;80:106210.
38. Valentino L, Pierre J. JAK/STAT signal transduction: regulators and implication in hematological malignancies. Biochem Pharmacol 2006;71:713-21.
39. Inagaki-Ohara K, Kondo T, Ito M, Yoshimura A. SOCS, inflammation, and cancer. JAKSTAT 2013;2:e24053.
40. Tamiya T, Kashiwagi I, Takahashi R, Yasukawa H, Yoshimura A. Suppressors of cytokine signaling (SOCS) proteins and JAK/STAT pathways: regulation of T-cell inflammation by SOCS1 and SOCS3. Arterioscler Thromb Vasc Biol 2011;31:980-5.
41. Yin Y, Liu W, Dai Y. SOCS3 and its role in associated diseases. Hum Immunol 2015;76:775-80.
42. Heinrich PC, Behrmann I, Haan S, Hermanns HM, Muller-Newen G, Schaper F. Principles of interleukin (IL)-6-type cytokine signalling and its regulation. Biochem J 2003;374:1-20.
43. Hjazi A, Obaid RF, Ali SS, Abdullaev B, Alsaab HO, Huldani H, et al. The cross-talk between LncRNAs and JAK-STAT signaling pathway in cancer. Pathol Res Pract 2023;248:154657.
44. Keewan E, Matlawska-Wasowska K. The emerging role of suppressors of cytokine signaling (SOCS) in the development and progression of leukemia. Cancers (Basel) 2021;13:4000.
45. Himpe E, Kooijman R. Insulin-like growth factor-I receptor signal transduction and the Janus kinase/signal transducer and activator of transcription (JAK-STAT) pathway. Biofactors 2009;35:76-81.
46. Chikuma S, Kanamori M, Mise-Omata S, Yoshimura A. Suppressors of cytokine signaling: potential immune checkpoint molecules for cancer immunotherapy. Cancer Sci 2017;108:574-80.

Online Supplementary Material:

Supplementary Figure S1. The miR-34a/SOCS3 axis regulates the M2 polarization of macrophages and affects the malignant process of PANC-1 cells.

Received: 24 December 2024. Accepted: 2 April 2025.

European Journal of Histochemistry 2025; 69:4176
doi:10.4081/ejh.2025.4176